 

https://doi.org/10.1070/QEL17035

# Stimulated emission, photoluminescence, and localisation of nonequilibrium charge carriers in ultrathin (monolayer) GaN/AlN quantum wells

E.V. Lutsenko, M.V. Rzheutski, A.V. Nagorny, A.V. Danilchyk, D.V. Nechaev, V.N. Jmerik, S.V. Ivanov

*Abstract.* **The stimulated emission and photoluminescence of ultrathin GaN quantum wells with a nominal thickness of 1.5–2 monolayers (MLs) and AlN barrier layers 4–6.66 ML thick, obtained by plasma-activated molecular beam epitaxy on c-sapphire substrates, are studied. The stimulated emission of TE polarisation in ultrathin GaN/AlN quantum wells is obtained under pumping directly into quantum wells. The wavelength of stimulated emission varied from 262 to 290 nm, depending on the thickness of the wells and barriers. It is shown that stimulated emission is achieved on localised GaN states with a thickness of 2 and 3 ML in ultrathin quantum wells with a nominal thickness of 1.5 and 2 ML, respectively. The minimum excitation threshold of stimulated emission was 700 kW cm$^{-2}$ at $\lambda$ = 270 nm.**

***Keywords:*** *optical pumping, ultraviolet stimulated radiation, ultrathin GaN/AlN quantum wells, molecular beam epitaxy.*

## 1. Introduction

In recent years, active studies of wide-gap nitride compounds $A^3N$ and the rapid development of instrumentation technologies based on them gave rise to the massive introduction of high-efficiency LED lighting and the industrial production of high-power injection lasers emitting in the violet–green region of the spectrum.

The use of such injection lasers for pumping active laser media made it possible to develop not only solid-state [1, 2], but also diode-pumped semiconductor lasers [3–5], in which there is no need in second-harmonic generation. In addition, technological progress in growth of GaN-based compounds has launched a new stage in the development of microwave electronics. Currently, more than half of the production of solid-state microwave electronics is produced based on the heterostructures of these compounds. In addition, in the near future, a massive transition is expected from traditional devices based on Si and SiC to new, more efficient devices based on $A^3N$ compounds for power electronics.

**E.V. Lutsenko, M.V. Rzheutski, A.V. Nagorny, A.V. Danilchyk** Institute of Physics, National Academy of Sciences of Belarus, prosp. Nezavisimosti 68/2, 220072 Minsk, Belarus;
**D.V. Nechaev, V.N. Jmerik, S.V. Ivanov** Ioffe Institute, Politekhnicheskaya ul. 26, 194021 St. Petersburg, Russia;
e-mail: jmerik@pls.ioffe.ru

Received 4 April 2019
*Kvantovaya Elektronika* **49** (6) 535–539 (2019)
Translated by V.L. Derbov

Further development of optoelectronics, high frequency and power electronics is associated with AlN. The use of AlN-based heterostructures in optoelectronics leads to the development of ultraviolet LEDs and lasers. In microwave and power electronics, it provides a significant increase in frequencies, breakdown voltages, operating currents and power. In the active regions of most of these devices, the key role is played by AlGaN layers, for the formation of which simultaneous feeding of growth fluxes of all three elements is used. In this case, as a rule, significant fluctuations in the composition of the ternary compound are observed. In optoelectronic devices, this leads to a broadening of the spectral emission bands, while in microwave devices, there is a decrease in the mobility of charge carriers and a significant, by an order of magnitude, decrease in thermal conductivity. Among the various methods for reducing composition fluctuations in AlGaN compounds, the development of technologies for the growth of short-period AlN/GaN superlattices, which in the case of single-layer thicknesses are called digital or discrete solid solutions, is considered a promising direction [6–8]. The use of ultrathin GaN quantum wells (QWs) causes their pseudomorphic growth on AlN barrier layers (with crystallographic mismatch of these layers, 2.4%), and the spatial localisation of electrons and holes in ultrathin QWs does not lead to a significant separation of the positions of the maxima of the wave functions of these particles, which arises as a result of the action of internal electric fields (quantum-dimensional Stark effect) and can be quite significant for large QW thicknesses. This ensures high efficiency of radiative recombination of carriers and the absence of a red shift of the wavelength of the output radiation. As theoretically shown in Ref. [9], when the thickness of the ultrathin GaN QW varies from 1 to 4 monolayers (MLs), the effective band gap can vary from ~5.51 to ~3.81 eV, which corresponds to wavelengths from ~225 to ~325 nm.

In this work, we study photoluminescence (PL), stimulated emission (SE), and localisation of nonequilibrium charge carriers in heterostructures with multiple ultrathin GaN/AlN QWs, which are promising for producing active regions of optoelectronic devices and UV lasers.

## 2. Experiment

Heterostructures were grown on a plasma-activated molecular beam epitaxy setup Compact21T on annealed and nitrided c-$AL_2O_3$ substrates, on which nucleation layers of AlN were grown with a thickness of 65 nm [10]. Then using metal-modulated epitaxy, AlN buffer layers were grown up to 2 μm thick

[11] at a temperature of 780 °C under metal-enriched conditions with a ratio of metal (Al) and nitrogen fluxes of 1.2. To filter threading dislocations, ultrathin (3 nm thick) GaN layers were introduced into the buffer layer [12]. The upper part of the AlN buffer layer with a thickness of 250 nm was grown with the continuous supply of growth-supporting fluxes. At the same time, a layer of excess metal (Al) accumulated on the surface with a nominal thickness of no greater than ~50 ML reacted with a flux of nitrogen after the layer grew, forming AlN. Further growth of multiple GaN/AlN QWs was carried out at a constant substrate temperature of 700 °C. The main feature of the growth of GaN/AlN heterostructures was the use of a continuous flux of Ga ($F_{Ga}$ = 1 ML s$^{-1}$) with a pulsed flux of Al, $F_{Al}$ = 0.48 ML s$^{-1}$. Since the Al flux was slightly larger than the nitrogen flux ($F_N$ = 0.47 ML s$^{-1}$), this ensured the absence of Ga incorporation during the growth of AlN barrier layers [13]. In addition, the use of metal-enriched conditions for the growth of both the GaN QW and AlN barrier layers made it possible to calculate their nominal thicknesses based only on the nitrogen flux. Figure 1 shows the schematic images of the three studied heterostructures A, B, C, which consisted of sixty QWs with thicknesses 1.5 or 2 ML, the thickness of barrier layers ranging from 4 to 6.66 ML.

The growth rates of the layers and the morphology of their surfaces were controlled *in situ* using laser interferometry and reflected high-energy electron diffraction (RHEED), respectively. To characterise the structural quality of the grown structures, X-ray diffraction analysis and atomic force microscopy were used.

The PL and stimulated emission of ultrathin GaN/AlN quantum wells were investigated using the fifth harmonic of an Nd:YAG laser [$\lambda_{exc}$ = 213 nm, $I_{exc}$ ≈ 0.1 (PL) and ~0.1–10 MW cm$^{-2}$ (SE)] as an excitation source. Stimulated emission was obtained in the transverse measurement geometry, in which the radiation of the exciting laser was focused on the surface of the heterostructure into a strip with a size of 100 μm × 2 mm, oriented perpendicular to the cleaved facet. The SE parameters were specially measured without making a Fabry–Perot resonator in order to exclude the accidental influence of the quality of the mirrors of the resonator formed by cleavages on the threshold intensity of the exciting radiation. When measuring spectra using a MayaPro spectrometer (Ocean Optics), the registration of the PL spectrum and the SE was performed from the surface and the end of the heterostructure, respectively.

## 3. Results and discussion

Using the values of half-widths of symmetric and skew-symmetric reflections obtained from X-ray diffraction measurements, we estimated the density of threading screw and edge dislocations in AlN buffer layers as ~$4\times10^8$ and ~$5\times10^9$ cm$^{-2}$, respectively. Two-dimensional growth of GaN/AlN heterostructures was established from observations of RHEED line patterns during all the time of their growth and was confirmed by atomic force microscopy (AFM). The AFM studies showed atomic-smooth surface morphology with height of 1–2 ML and root-mean-square roughness of 0.8 nm, typical for spiral step growth on an area of 5 μm × 5 μm (details of the growth of these structures will be considered in a separate paper).

The PL spectra of all three studied heterostructures with multiple QWs are shown in Fig. 2. It can be seen that the PL spectra of ultrathin QWs consist of several bands, in contrast to those described in Refs [6–8], where only one maximum was observed in the spectra of 1.5 ML ultrathin GaN/AlN QWs. This is apparently due to different regimes of the QW growth. The emission spectrum of the heterostructure A comprises two bands with maxima at $\lambda$ = 239 and 259 nm, with the long-wavelength band being more intense. In the spectrum of the heterostructure B, three pronounced maxima are observed: at $\lambda$ = 242, 267 and 286 nm. Moreover, the second, most intense band of the heterostructure B is substantially shifted (by ~8 nm or ~140 meV) relative to the corresponding band of the heterostructure A. At the long-wavelength edge of the third band, a gentle tail is observed up to $\lambda \approx$ 350 nm. The two short-wavelength bands of the C heterostructure are low-intensity, and the third, most intense emission band, has a maximum at $\lambda$ = 289 nm. On its long-wavelength edge, there is an inflection, indicating the presence of another emission band. It should be noted that the authors of Ref. [14] also observed multicomponent PL spectra in ultrathin GaN/AlN QWs, but with a larger thickness of GaN (4–10 ML), individual bands of which were attributed to radiation from regions of wells with different thickness (number of layers).

It is interesting to compare the obtained results with the results of calculations [9] of the effective band gap of GaN/

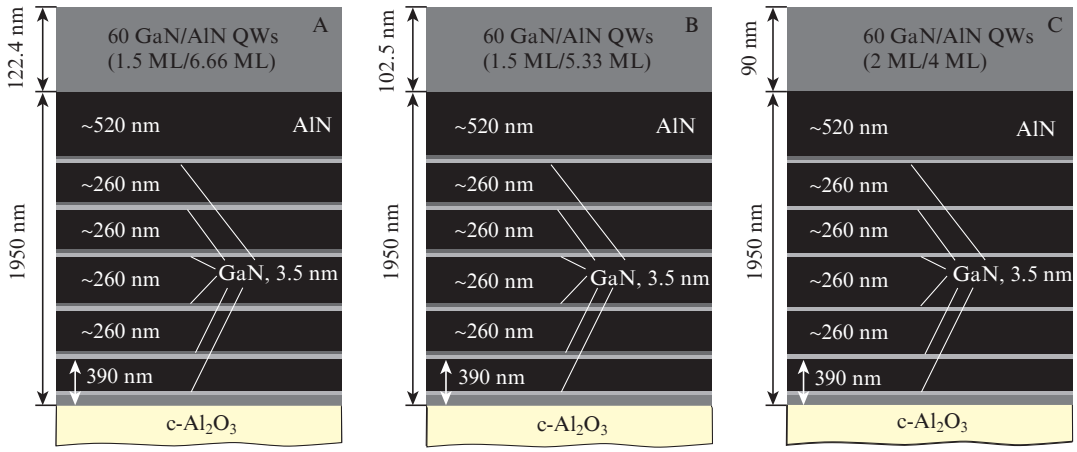


**Figure 1.** Schematic of heterostructures A, B, and C with multiple ultrathin GaN/AlN QWs.

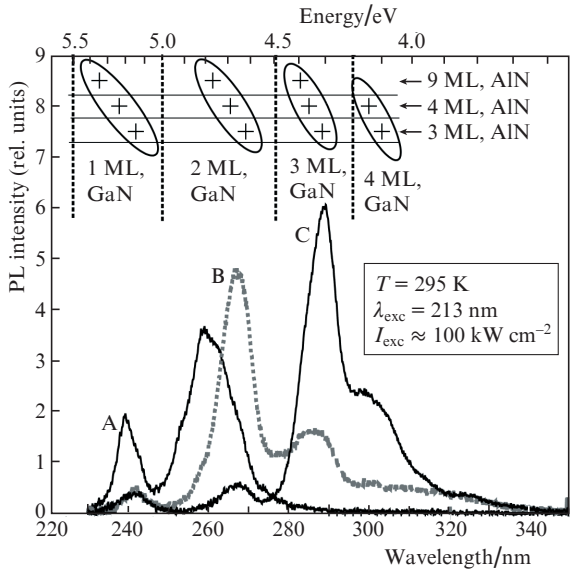


**Figure 2.** PL spectra of the heterostructures A, B, and C containing 60 ultrathin QWs (Fig. 1). The top shows the effective band gap values (+) for superlattices with varying widths of the GaN QW (1–4 ML) and AlN barrier layers (3–9 ML), calculated in Ref. [9].

AlN superlattices with different layer thicknesses. In addition to the experimental PL spectra, Fig. 2 also shows the results of these calculations for the thicknesses of the GaN QW and AlN barrier layers, which varied from 1 to 3 ML and from 3 to 9 ML, respectively. Their comparison with the position of the PL bands allows us to interpret the nature of these bands. Thus, the short-wavelength PL bands in all heterostructures can be interpreted as radiation from the most wide-bandgap QW regions with a minimum thickness of 1 ML. The relatively weak intensity of these bands is explained by the relatively small fraction of 1-ML-thick regions in the wells with a nominal thickness of 1.5–2 ML, as well as by the effective diffusion of non-equilibrium charge carriers in the region of the thicker wells. For example, in structures A, B with a nominal QW thickness of 1.5 ML, the maximum intensity is demonstrated by the bands related to radiation from QW regions with a thickness of 2 ML. The dominance in the PL spectra of these heterostructures of radiation from layers with a thickness of 2 ML indicates that these QW thickenings are not large and they are separated from each other by a distance comparable to the diffusion length of non-equilibrium charge carriers. The long-wavelength (by 140 meV) shift of the maximum of this band for the heterostructure B relative to the maximum for structure A is due to a decrease in the barrier thickness.

For heterostructure C with a nominal QW thickness of 2 ML the maximum intensity belongs to the band, the position of which corresponds to radiation from regions with a QW thickness of 3 ML, and the feature at the long-wavelength edge of this band is due to emission from a well with a thickness of 4 ML.

Some difference between the effective band gap and the position of the maxima of the PL bands is due to the exciton binding energy, quantum-dimensional effects associated with the limitation of the sizes of regions of different thickness [6–8], and fluctuations in the distance between these sections of the wells, which manifests itself in the presence of inflections in the emission spectra (particularly this is clearly seen in the PL spectra of the heterostructure A).

Thus, the dominant band in the PL spectrum of heterostructures with QWs with a nominal thickness of 1.5 ML is caused by recombination of nonequilibrium charge carriers in localised states created by QW thickenings up to 2 ML, and for QW with a nominal thickness 2 ML, thicknesses up to 3 ML.

Detection of localised states in QWs suggested the possibility of obtaining optical amplification and lasing with a relatively low threshold even when using optical pumping with $\lambda = 213$ nm, for which the barrier layer is transparent and the radiation is absorbed in the QW only. In GaN/AlN heterostructures grown on AlN/c-$AL_2O_3$ templates, the resonator mirrors produced by cleaving are of poor quality, and therefore the experiments were carried out without a second resonator face to minimise the influence of the quality of resonator mirrors on the threshold intensity.

The smallest threshold of stimulated emission was shown by heterostructure B, for which (see Fig. 3) a nonlinear increase in the PL intensity due to localised states 2 ML thick and a narrow peak of radiation at $\lambda = 270$ nm on the long-wavelength wing of the band near the maximum of spontaneous radiation intensity were observed with increasing pump power. From the dependence of the integrated PL intensity on the excitation intensity and the presence of a narrow peak on it, the SE threshold was estimated as ~700 kW cm$^{-2}$ at room temperature. Further increase in the intensity of the pump radiation led to a sharp increase in the intensity of the SE peak, and then to its broadening and long-wavelength shift. The SE had TE polarisation. Since the heterostructures were pumped not through the facing and barrier layers, but directly in the QW, the stimulated emission excitation threshold was relatively high and corresponded to the threshold for the best AlGaN epitaxial layers [15].

It can be assumed that by pumping into the cladding and barrier layers the threshold pump power can be significantly

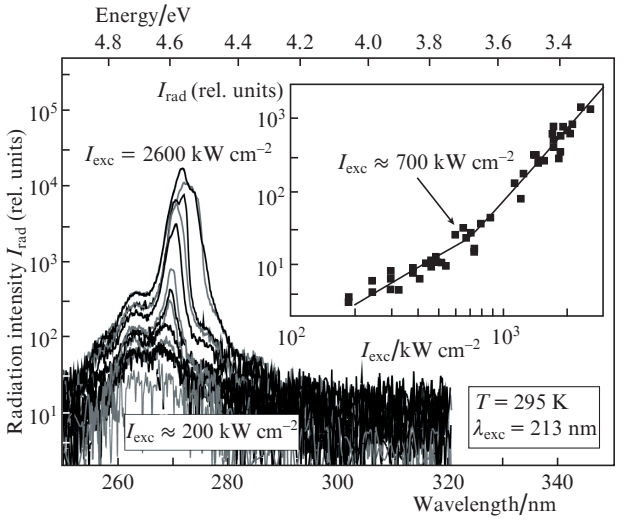


**Figure 3.** Emission spectra recorded from the end face of heterostructure B, at various transverse pump radiation intensities. The inset shows the integral intensity of radiation from the end of the heterostructure as a function of the intensity of excitation.

reduced to values corresponding to the best world results [16]. It is interesting to note that for the first time low-threshold generation of radiation in the spectral region of the UVB (range 315–280 nm according to the classification of CIE – the International Commission on Illumination) was achieved in the AlGaN QW formed precisely by inserts of ultrathin GaN layers in the AlGaN matrix [17] (the inserts had a thickness of 0.8 ML).

Investigations of heterostructure A showed that its SE characteristics are similar, but its wavelength, like the wavelength of spontaneous emission, was slightly shorter than for structure B, and amounted to 262 nm (Fig. 4). SE was also achieved on the long-wavelength wing of the dominant PL band near its maximum. The threshold intensity of SE excitation was 2500 kW cm$^{-2}$. As in the case of structure B, SE evolved on localised states in the QW region with a thickness of 2 ML. Thus, a decrease in the thickness of the AlN barrier layer from 6.66 to 5.33 ML resulted in a long-wavelength shift of the SE peak by 12 nm. Therefore, by varying the thickness of the barrier layer, it is possible to tune effectively (within small limits) the wavelength of radiation from lasers with an active region consisting of such ultrathin QWs.

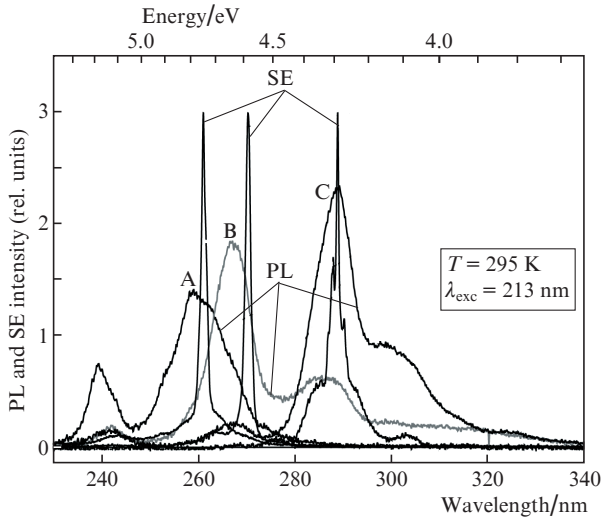


**Figure 4.** Stimulated emission spectra (at excitation intensities close to the threshold) and photoluminescence spectra recorded respectively from the end faces and from the surfaces of the A, B (2 ML GaN) and C (3 ML GaN) heterostructures.

Stimulated emission in heterostructure C was observed at an even longer wavelength, ~290 nm (Fig. 4). In this sample, the SE was achieved on localised states formed by thickenings of ultrathin QWs constituting 3 ML. Thus, the maximum shift of the SE spectrum for localised states with a thickness of 3 ML relative to localised states with a thickness of 2 ML was 28 nm (or 450 meV). As in the previous cases, the stimulated emission had TE polarisation, and the threshold excitation intensity was 1000 kW cm$^{-2}$, which slightly exceeds the minimum threshold for localised states with a thickness of 2 ML.

Apparently, the increased value of the SE excitation threshold for heterostructure A compared with the B and C heterostructures is due, first of all, to the worst transport of nonequilibrium charge carriers to localised states 2 ML thick, which is manifested in a rather intense emission from 1 ML regions of the ultrathin QW.

## 4. Conclusions

Thus, using plasma-activated molecular beam epitaxy, we demonstrated the production of ultrathin (monolayer) GaN quantum wells in an AlN matrix with localised states caused by fluctuations of the well thickness. Stimulated emission was obtained with $\lambda = 262-290$ nm and a minimum threshold excitation intensity of 700 kW cm$^{-2}$ ($\lambda = 270$ nm) in ultrathin GaN/AlN QWs grown on sapphire substrates. It is shown that stimulated emission is achieved in localised states caused by fluctuations in the thickness of the ultrathin GaN quantum wells. The low (700 kW cm$^{-2}$) threshold of stimulated emission under direct pumping into the QW is due to the effective diffusion of nonequilibrium charge carriers to localised states from regions of wells of smaller thickness. It is shown that a change in the thickness of the barriers and QWs makes it possible to vary the wavelength of stimulated emission and photoluminescence within wide limits.

***Acknowledgements.*** The work at the B.I. Stepanov Institute of Physics of the National Academy of Sciences of Belarus was carried out under the partial support of tasks 2.1.01 and 2.1.04 of the State Programme of Research and Development "Photonics, Opto- and Microelectronics". The research at the Ioffe Institute was partially supported by the RFBR-BRICS (No. 17-52-278980089).

## References

1. Kränkel C., Marzahl D.-T., Moglia F., Huber G., Metz P.W. *Las. Photon. Rev.*, **10**, 548 (2016).
2. Sawai S., Hosaka A., Kawauchi H., Hirosawa K., Kannari F. *Appl. Phys. Express*, **7**, 022702 (2014).
3. Lutsenko E.V., Voinilovich A.G., Rzheutskii V.N., Pavlovski N.V., Yablonskii G.P., Sorokin S.V., Gronin S.V., Sedova I.V., Kopiev P.S., Ivanov S.V., Alanzi M., Khamidalddin A., Aliamani A. *Quantum Electron.*, **43**, 418 (2013) [*Kvantovaya Elektron.*, **43**, 418 (2013)].
4. Sorokin S.V., Gronin S.V., Sedova I.V., Rakhlin M.V., Baidakova M.V., Kop'ev P.S., Vainilovich A.G., Lutsenko E.V., Yablonskii G.P., Gamov N.A., Zhdanova E.V., Zverev M.M., Ruvimov S.S., Ivanov S.V. *Semiconductors*, **49**, 331 (2015).
5. Alyamani A., Lutsenko E.V., Gronin S.V., Vainilovich A.G., Pavlovskii V.N., Yablonskii G.P., Tarasuk N.P., Aljohani M., Aljariwi A., Sorokin S.V., Sedova I.V., Ivanov S.V. *Phys. Stat. Sol.*, **253**, 1490 (2016).
6. Islam S.M., Lee K., Verma J., Protasenko V., Rouvimov S., Bharadwaj S., Xing H., Jena D. *Appl. Phys. Lett.*, **110**, 041108 (2017).
7. Islam S.M., Protasenko V., Lee K., Rouvimov S., Verma J., Xing H., Jena D. *Appl. Phys. Lett.*, **111**, 091104 (2017).
8. Bayer D., Islam S.M., Jones C.M., Protasenko V., Jena D., Kioupakis E. *Appl. Phys. Lett.*, **109**, 241102 (2016).
9. Sun W., Tan C.-K., Tansu N. *Sci. Reports*, **7**, 11826 (2017).
10. Nechaev D.V., Aseev P.A., Jmerik V.N., Brunkov P.N., Kuznetsova Y.V., Sitnikova A.A., Ratnikov V.V., Ivanov S.V. *J. Cryst. Growth*, **378**, 319 (2013).
11. Jmerik V.N., Mizerov A.M., Nechaev D.V., Aseev P.A., Sitnikova A.A., Troshkov S.I., Kop'ev P.S., Ivanov S.V. *J. Cryst. Growth*, **354**, 188 (2012).
12. Jmerik V.N., Lutsenko E.V., Ivanov S.V. *Phys. Stat. Sol. A*, **210**, 439 (2013).

13. Jmerik V.N., Nechaev D.V., Ivanov S.V., in *Molecular Beam Epitaxy (MBE): From Research to Mass Production.* Ed. by M. Henini (Elsevier, 2018) Ch. 8.
14. Kandaswamy P.K., Guillot F., Bellet-Amalric E., Monroy E., Nevou L., Tchernycheva M., Michon A., Julien F.H., Baumann E., Giorgetta F.R., Hofstetter D., Remmele T., Albrecht M., Birner S., Dang L.S. *J. Appl. Phys*., **104**, 093501 (2008).
15. Li X.-H., Detchprohm T., Kao T.-T., Satter Md.M., Shen S.-C., Yoder P.D., Dupuis R.D., Wang S., Wei Y.O., Xie H., Fischer A.M., Ponce F.A., et al. *Appl. Phys. Lett*., **105**, 141106 (2014).
16. Lutsenko E.V., Rzheutskii N.V., Voinilovich A.G., Svitenkov I.E., Nagornyi A.V., Shulenkova V.A., Yablonskii G.P., Alekseev A.N., Petrov S.I., Solov'ev Ya.A., Petlitskii A.N., Zhigulin D.V., Solodukha V.A. *Quantum Electron*., **49**, 540 (2019) [*Kvantovaya Elektron*., **49**, 540 (2019)].
17. Jmerik V.N., Mizerov A.M., Sitnikova A.A., Kop'ev P.S., Ivanov S.V., Lutsenko E.V., Tarasuk N.P., Rzheutskii N.V., Yablonskii G.P. *Appl. Phys. Lett*., **96**, 141112 (2010).